



Bulk Geochemistry of the Sand Fraction from CRP-3 (Victoria Land Basin, Antarctica): Evidence for Provenance and Milankovitch Climatic Fluctuations

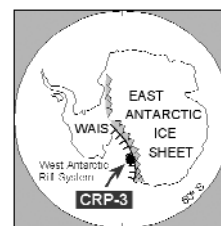
M. SPROVIERI*, A. BELLANCA & R. NERI

Dipartimento di Chimica e Fisica della Terra ed Applicazioni alle Georisorse e ai Rischi Naturali (CFTA), Università di Palermo
90123 Palermo, Italy

Received 9 January 2001; accepted in revised form 6 November 2001

Abstract - A total of 167 samples distributed throughout the CRP-3 drillhole from 5.77 to 787.68 mbsf and representing fine to coarse sandstones have been analysed by X-ray fluorescence spectrometry (XRF). Bulk sample geochemistry (major and trace elements) indicates a dominant provenance of detritus from the Ferrar Supergroup in the uppermost 200 mbsf of the core. A markedly increased contribution from the Beacon sandstones is recognized below 200 mbsf and down to 600 mbsf. In the lower part of CRP-3, down to 787.68 mbsf, geochemical evidence for influxes of Ferrar materials is again recorded.

On the basis of preliminary magnetostratigraphic data reported for the lower 447 mbsf of the drillhole, we tentatively evaluated the main periodicities modulating the geochemical records. Our results identify a possible influence of the precession, obliquity and long-eccentricity astronomical components (21, 41, and 400 ky frequency bands) on the deposition mechanisms of the studied glaciomarine sediments.



INTRODUCTION

This paper presents the results of major and trace element analyses performed on fine to coarse sandstones from the CRP-3 drillhole. These results have been discussed to assess the sediment provenance and processed by spectral analysis to test the presence of cyclic patterns in the geochemical records.

When biostratigraphic and magnetostratigraphic constrains are poorly defined, the recognition of statistically significant periodicities in sedimentary records related to astronomical/orbital forcing may be useful to calibrate the time interval of the studied succession (House, 1995).

By analysing physical properties of mudstone and fine-grained sandstone intervals in CRP-2/2A drillhole, Niessen et al. (2000), Cape Roberts Science Team (1999), and Claps et al. (2000) identified high-frequency periodicities which the authors correlated to the Milankovitch periodic orbital forcing. Interesting cyclostratigraphic results have also been obtained for the upper 200 mbsf of the CRP-3 core. Based on combined spectral methodologies, it has been suggested the presence of the three classic Milankovitch periodicities modulating the magnetic susceptibility in this part of the core (Cape Roberts Science Team, 2000).

These results stimulated us to use a similar approach for testing cyclicity in the geochemical

records from the lower part of the CRP-3. While a relatively reliable time framework for the upper part of the CRP-3 core is provided by a good biostratigraphic and magnetostratigraphic control, only approximate temporal constrains are available for the 350 to 789.77 mbsf interval (Cape Roberts Science Team, 2000). Then, the recognition of selected periodicities in the geochemical signals could represent a useful tool to calibrate the time record of the lower part of the CRP-3 core, ascribed to the early Oligocene. Furthermore, the recognition of specific frequency bands related to well-known climatic influences could give the opportunity to study modes and times of possible response of the Oligocene East Antarctic Ice Sheet.

SAMPLES AND PROCESSING

Analyses were performed on 167 sand-grained samples scattered throughout the drillhole from 5.77 to 787.68 mbsf, with a mean distribution of one sample every 5 m.

Si, Ti, Al, Fe, Mn, Mg, Ca, Na, K, P and Cr, Ba, La, Ce, V, Zr, Nb, Y, Sr, Rb, Ni were determined by X-ray fluorescence spectrometry (XRF) on pressed, boric-acid backed pellets of bulk rock. Data reduction was achieved using the method described by Franzini et al. (1975). Certified reference materials were used as monitors of data quality. Analytical errors were

below 1% for Si, Al, Na; below 3% for Ti, K, Fe, Ca; and below 10% for Mg, Mn, P and trace elements. All samples were washed repeatedly in deionized water prior to analysis to avoid contamination resulting from drilling mud and seawater.

RESULTS AND DISCUSSION

Major and minor element analyses of CRP-3 samples are given in tables 1 and 2 and in figures 1 and 2. The data plotted in the figures are normalized to 100% L.O.I. (Loss On Ignition)-free. In order to discuss the geochemical results in terms of provenance, we assume that, as for the previously studied CRP-1 and CRP-2/2A sequences, main sources for sediments in CRP-3 are the Transantarctic

Mountains (TAM) with quartzose sandstones of the Devonian-Triassic Beacon Supergroup, Jurassic dolerites and Kirkpatrick basalts, coarse-grained plutonic rocks (Cambro-Ordovician Granite Harbour Intrusive Complex), and minor metamorphic rocks from the Upper Proterozoic basement.

DEPTH PROFILES

The depth profile of SiO₂ (Fig. 1) exhibits a marked increase of the element below approximately 160 mbsf. Despite of wide fluctuations, SiO₂ concentrations remain high, generally greater than 80%, throughout a thick interval of the drillhole down to about 600 mbsf. Below 600 mbsf, SiO₂ clearly decreases. The overall very high contents of SiO₂ are indicative of strong influxes of detritus from the Beacon sandstones throughout most of CRP-3. Higher

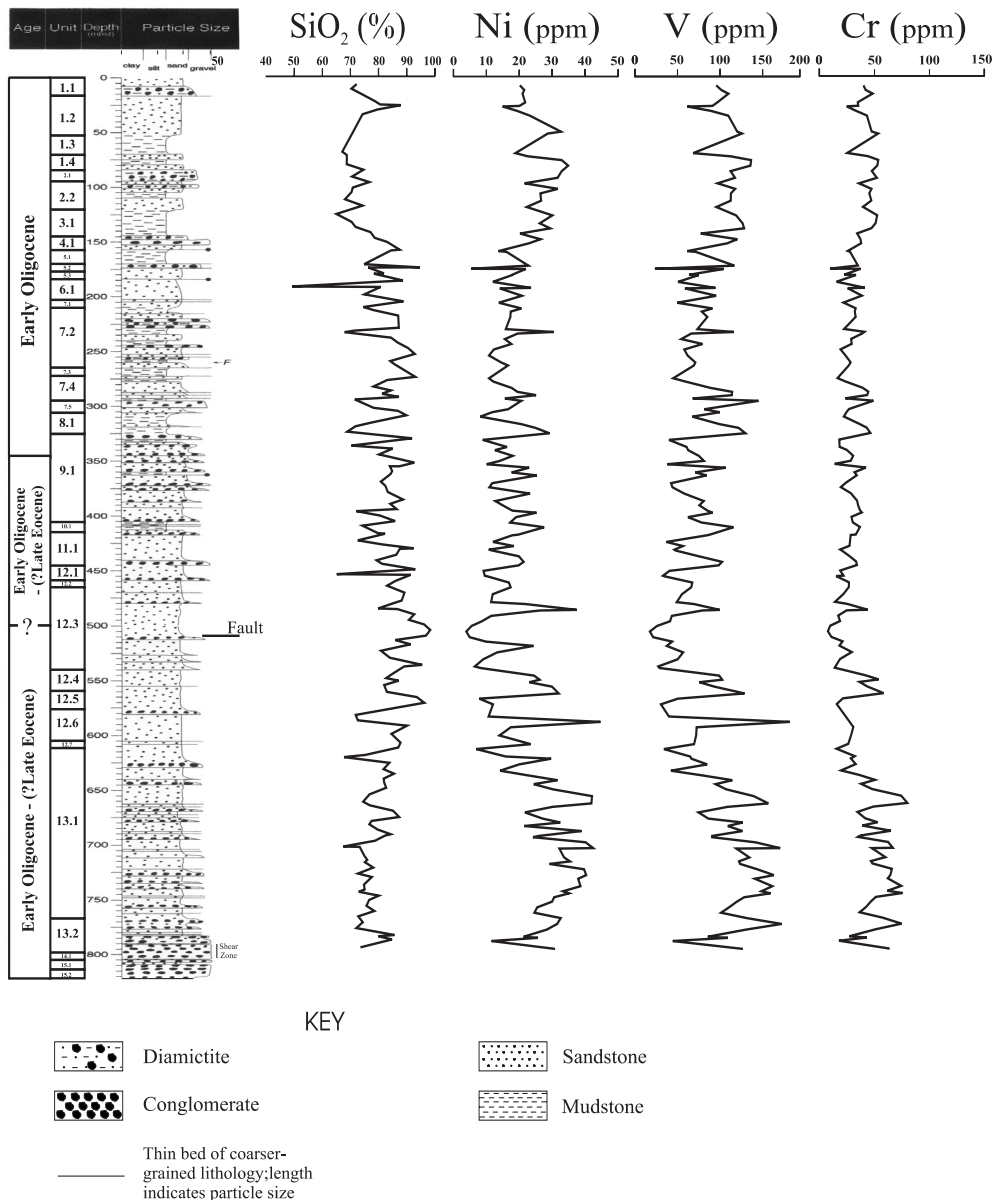


Fig. 1 - CRP-3 lithologic section with depth profiles for SiO₂, Ni, V, and Cr.

Tab. 1 - Major element concentrations (wt%) of CRP-3 samples. Data listed are normalised to 100% (hydrous basis).

| Depth | SiO ₂ | TiO ₂ | Al ₂ O ₃ | Fe ₂ O ₃ | MnO | MgO | CaO | Na ₂ O | K ₂ O | P ₂ O ₅ | L.O.I |
|--------|------------------|------------------|--------------------------------|--------------------------------|------|------|-------|-------------------|------------------|-------------------------------|-------|
| 5.77 | 71.24 | 0.48 | 10.51 | 3.59 | 0.07 | 2.52 | 2.60 | 4.26 | 2.14 | 0.09 | 2.49 |
| 9.90 | 69.30 | 0.52 | 10.52 | 4.88 | 0.08 | 2.76 | 3.86 | 2.11 | 2.16 | 0.10 | 3.71 |
| 13.26 | 71.89 | 0.56 | 10.96 | 4.32 | 0.08 | 2.81 | 2.66 | 2.12 | 2.21 | 0.09 | 2.31 |
| 21.16 | 77.99 | 0.41 | 8.38 | 3.75 | 0.07 | 2.20 | 2.82 | 1.13 | 1.34 | 0.08 | 1.82 |
| 24.32 | 80.02 | 0.37 | 7.85 | 3.44 | 0.07 | 2.16 | 2.72 | 1.03 | 1.25 | 0.07 | 1.03 |
| 24.88 | 87.75 | 0.20 | 3.97 | 2.32 | 0.06 | 1.22 | 1.81 | 0.86 | 0.68 | 0.04 | 1.09 |
| 28.80 | 78.98 | 0.36 | 7.44 | 3.26 | 0.08 | 2.10 | 2.82 | 1.73 | 1.22 | 0.07 | 1.93 |
| 33.14 | 73.42 | 0.53 | 10.74 | 4.38 | 0.07 | 2.78 | 3.08 | 1.39 | 1.77 | 0.09 | 1.75 |
| 47.61 | 70.24 | 0.68 | 12.09 | 4.68 | 0.08 | 2.94 | 3.36 | 1.74 | 2.27 | 0.13 | 1.78 |
| 49.40 | 69.83 | 0.62 | 11.91 | 5.04 | 0.08 | 2.96 | 2.97 | 1.47 | 2.06 | 0.10 | 2.98 |
| 67.03 | 65.92 | 0.26 | 7.00 | 12.08 | 0.06 | 1.92 | 2.09 | 1.05 | 0.91 | 0.06 | 8.65 |
| 69.97 | 67.58 | 0.48 | 9.94 | 4.62 | 0.11 | 2.96 | 7.16 | 1.34 | 1.53 | 0.11 | 4.18 |
| 73.40 | 67.62 | 0.62 | 12.50 | 5.68 | 0.09 | 3.47 | 3.97 | 1.41 | 2.03 | 0.11 | 2.50 |
| 78.35 | 67.59 | 0.61 | 12.56 | 5.75 | 0.09 | 3.70 | 3.57 | 1.56 | 2.12 | 0.10 | 2.35 |
| 83.39 | 73.82 | 0.50 | 10.13 | 4.43 | 0.08 | 3.24 | 3.23 | 1.35 | 1.79 | 0.09 | 1.34 |
| 89.47 | 69.55 | 0.55 | 11.38 | 4.67 | 0.08 | 3.41 | 4.14 | 1.39 | 2.11 | 0.09 | 2.63 |
| 94.47 | 75.94 | 0.38 | 7.74 | 3.22 | 0.09 | 2.28 | 4.73 | 1.40 | 1.26 | 0.07 | 2.88 |
| 99.47 | 69.78 | 0.55 | 11.64 | 5.13 | 0.08 | 4.39 | 2.55 | 1.72 | 2.22 | 0.09 | 1.85 |
| 103.58 | 69.39 | 0.54 | 11.53 | 4.72 | 0.08 | 3.69 | 2.61 | 1.88 | 2.25 | 0.10 | 3.22 |
| 110.16 | 66.89 | 0.55 | 11.90 | 5.13 | 0.10 | 4.10 | 3.65 | 1.85 | 2.34 | 0.10 | 3.39 |
| 115.87 | 73.41 | 0.45 | 10.42 | 3.93 | 0.08 | 3.22 | 2.19 | 1.78 | 1.74 | 0.07 | 2.71 |
| 123.42 | 63.73 | 0.61 | 12.34 | 5.38 | 0.10 | 3.79 | 5.25 | 1.85 | 2.56 | 0.11 | 4.28 |
| 130.57 | 69.37 | 0.57 | 11.64 | 5.24 | 0.08 | 4.26 | 1.84 | 1.59 | 2.16 | 0.08 | 3.19 |
| 135.15 | 70.87 | 0.58 | 11.49 | 4.83 | 0.08 | 3.32 | 2.00 | 1.67 | 2.17 | 0.08 | 2.92 |
| 139.88 | 76.44 | 0.28 | 6.01 | 3.00 | 0.14 | 1.91 | 5.33 | 1.93 | 0.75 | 0.04 | 4.17 |
| 145.09 | 77.99 | 0.38 | 5.93 | 4.73 | 0.08 | 3.76 | 3.56 | 1.29 | 0.75 | 0.05 | 1.48 |
| 148.73 | 82.62 | 0.31 | 4.99 | 3.90 | 0.07 | 3.44 | 1.69 | 1.15 | 0.76 | 0.04 | 1.04 |
| 155.82 | 87.25 | 0.21 | 4.61 | 1.71 | 0.06 | 2.50 | 1.04 | 1.24 | 0.76 | 0.03 | 0.59 |
| 156.52 | 84.01 | 0.23 | 5.42 | 1.97 | 0.06 | 2.76 | 1.33 | 1.30 | 0.95 | 0.03 | 1.95 |
| 168.94 | 74.01 | 0.53 | 9.53 | 4.19 | 0.08 | 3.99 | 1.96 | 1.73 | 1.74 | 0.09 | 2.15 |
| 171.75 | 94.80 | 0.05 | 0.85 | 0.58 | 0.06 | 0.22 | 1.06 | 0.16 | 0.24 | 0.01 | 1.98 |
| 171.95 | 75.58 | 0.43 | 8.29 | 4.01 | 0.07 | 4.49 | 1.54 | 2.06 | 1.48 | 0.06 | 1.98 |
| 177.19 | 81.41 | 0.25 | 5.46 | 2.54 | 0.07 | 2.89 | 2.75 | 1.33 | 1.11 | 0.07 | 2.11 |
| 177.47 | 77.66 | 0.30 | 7.57 | 2.38 | 0.07 | 3.30 | 2.51 | 2.50 | 1.26 | 0.08 | 2.36 |
| 183.66 | 88.50 | 0.19 | 3.92 | 1.65 | 0.06 | 1.95 | 0.79 | 1.02 | 0.77 | 0.04 | 1.11 |
| 189.16 | 47.29 | 0.46 | 9.41 | 4.52 | 0.23 | 3.43 | 16.25 | 1.28 | 2.07 | 0.29 | 14.77 |
| 189.51 | 80.19 | 0.22 | 6.07 | 4.36 | 0.05 | 1.54 | 0.67 | 1.44 | 1.16 | 0.04 | 4.27 |
| 196.27 | 74.16 | 0.43 | 9.99 | 3.89 | 0.07 | 4.08 | 0.90 | 1.64 | 2.27 | 0.06 | 2.51 |
| 202.56 | 88.67 | 0.18 | 4.17 | 1.55 | 0.06 | 1.76 | 0.60 | 0.99 | 0.96 | 0.03 | 1.02 |
| 207.68 | 73.76 | 0.28 | 7.58 | 3.17 | 0.08 | 5.17 | 2.12 | 1.86 | 1.59 | 0.04 | 4.34 |
| 210.49 | 77.68 | 0.30 | 6.86 | 2.52 | 0.07 | 3.88 | 2.34 | 1.82 | 1.34 | 0.04 | 3.15 |
| 215.39 | 86.73 | 0.30 | 4.08 | 2.56 | 0.06 | 2.64 | 1.08 | 1.04 | 0.76 | 0.03 | 0.71 |
| 226.39 | 86.98 | 0.23 | 3.59 | 2.50 | 0.06 | 2.06 | 1.69 | 0.72 | 0.75 | 0.04 | 1.39 |
| 229.00 | 70.71 | 0.47 | 11.38 | 4.64 | 0.07 | 3.84 | 1.03 | 1.69 | 2.48 | 0.06 | 3.64 |
| 230.42 | 66.82 | 0.23 | 5.07 | 1.70 | 0.13 | 1.52 | 13.57 | 1.22 | 1.12 | 0.03 | 8.59 |
| 235.47 | 84.10 | 0.17 | 3.30 | 1.43 | 0.08 | 0.93 | 4.92 | 0.80 | 0.79 | 0.02 | 3.46 |
| 239.86 | 86.55 | 0.23 | 5.35 | 2.10 | 0.05 | 1.85 | 0.64 | 0.81 | 1.31 | 0.03 | 1.07 |
| 244.83 | 90.43 | 0.17 | 3.29 | 1.91 | 0.05 | 1.13 | 0.54 | 0.66 | 0.59 | 0.03 | 1.19 |
| 250.24 | 92.89 | 0.17 | 2.74 | 1.36 | 0.05 | 0.70 | 0.35 | 0.51 | 0.59 | 0.02 | 0.62 |
| 256.63 | 83.78 | 0.28 | 6.10 | 2.04 | 0.07 | 1.04 | 2.34 | 0.81 | 1.67 | 0.04 | 1.83 |
| 259.30 | 85.25 | 0.28 | 6.35 | 1.74 | 0.06 | 0.83 | 1.15 | 0.75 | 1.66 | 0.04 | 1.90 |
| 270.94 | 93.05 | 0.13 | 2.70 | 0.92 | 0.05 | 0.35 | 0.42 | 0.66 | 0.61 | 0.02 | 1.09 |
| 273.85 | 82.69 | 0.22 | 4.52 | 1.62 | 0.08 | 0.54 | 4.77 | 0.71 | 1.07 | 0.03 | 3.75 |
| 279.65 | 77.56 | 0.27 | 4.87 | 2.27 | 0.08 | 1.10 | 7.31 | 0.84 | 1.06 | 0.03 | 4.60 |
| 283.21 | 83.99 | 0.33 | 5.85 | 2.62 | 0.06 | 1.40 | 1.63 | 1.19 | 1.18 | 0.03 | 1.72 |
| 286.19 | 80.75 | 0.33 | 6.83 | 3.25 | 0.06 | 2.59 | 1.80 | 1.15 | 1.55 | 0.03 | 1.65 |
| 289.17 | 87.04 | 0.21 | 3.23 | 2.11 | 0.07 | 0.73 | 3.28 | 0.62 | 0.56 | 0.03 | 2.13 |
| 291.40 | 70.55 | 0.36 | 4.28 | 3.59 | 0.11 | 2.10 | 11.51 | 0.75 | 0.68 | 0.03 | 6.03 |
| 298.96 | 77.55 | 0.22 | 3.42 | 4.92 | 0.10 | 3.21 | 8.74 | 0.68 | 0.68 | 0.03 | 0.44 |
| 301.64 | 86.63 | 0.22 | 4.23 | 3.65 | 0.06 | 1.28 | 0.83 | 0.69 | 0.94 | 0.03 | 1.45 |
| 305.71 | 89.70 | 0.18 | 3.58 | 1.85 | 0.06 | 0.82 | 1.24 | 0.59 | 0.82 | 0.03 | 1.14 |
| 312.35 | 76.84 | 0.36 | 8.72 | 3.36 | 0.07 | 3.71 | 1.22 | 1.36 | 2.48 | 0.04 | 1.83 |
| 315.74 | 70.82 | 0.50 | 10.30 | 5.21 | 0.08 | 5.28 | 1.15 | 1.72 | 2.24 | 0.07 | 2.63 |
| 320.60 | 67.82 | 0.59 | 12.16 | 5.64 | 0.08 | 5.11 | 1.15 | 2.01 | 2.67 | 0.07 | 2.70 |
| 326.64 | 91.89 | 0.16 | 3.02 | 1.23 | 0.06 | 1.42 | 0.21 | 0.47 | 0.85 | 0.02 | 0.67 |
| 333.16 | 69.35 | 0.16 | 2.90 | 1.92 | 0.05 | 2.28 | 1.34 | 0.68 | 0.63 | 0.02 | 20.67 |
| 335.93 | 84.64 | 0.18 | 3.28 | 2.11 | 0.07 | 3.07 | 3.07 | 0.64 | 0.75 | 0.02 | 2.17 |
| 341.11 | 79.64 | 0.28 | 5.01 | 2.84 | 0.07 | 2.57 | 4.30 | 0.68 | 1.41 | 0.04 | 3.16 |
| 345.73 | 87.79 | 0.27 | 5.16 | 3.00 | 0.06 | 0.68 | 0.75 | 0.77 | 0.99 | 0.05 | 0.49 |
| 348.67 | 92.71 | 0.12 | 2.30 | 1.24 | 0.05 | 0.36 | 1.38 | 0.31 | 0.46 | 0.02 | 1.04 |

Tab. 1 - Continued.

| Depth | SiO ₂ | TiO ₂ | Al ₂ O ₃ | Fe ₂ O ₃ | MnO | MgO | CaO | Na ₂ O | K ₂ O | P ₂ O ₅ | L.O.I |
|--------|------------------|------------------|--------------------------------|--------------------------------|------|------|-------|-------------------|------------------|-------------------------------|-------|
| 351.85 | 87.20 | 0.29 | 4.81 | 0.02 | 0.06 | 3.09 | 0.74 | 1.03 | 0.99 | 0.03 | 1.74 |
| 351.85 | 83.61 | 0.27 | 4.70 | 3.98 | 0.05 | 3.03 | 0.70 | 0.96 | 0.92 | 0.03 | 1.74 |
| 356.15 | 84.46 | 0.21 | 5.82 | 2.69 | 0.06 | 2.41 | 0.84 | 1.00 | 1.45 | 0.03 | 1.03 |
| 358.92 | 83.88 | 0.24 | 5.01 | 2.90 | 0.06 | 2.72 | 1.43 | 0.89 | 1.29 | 0.04 | 1.54 |
| 365.84 | 80.23 | 0.15 | 2.68 | 1.33 | 0.08 | 1.12 | 7.86 | 0.38 | 0.71 | 0.02 | 5.42 |
| 369.61 | 81.98 | 0.12 | 2.12 | 1.57 | 0.08 | 1.16 | 7.13 | 0.33 | 0.44 | 0.02 | 5.05 |
| 375.29 | 82.83 | 0.13 | 2.18 | 1.89 | 0.08 | 0.54 | 7.40 | 0.32 | 0.41 | 0.02 | 4.19 |
| 381.97 | 88.46 | 0.18 | 3.95 | 2.75 | 0.05 | 0.66 | 1.07 | 0.57 | 0.77 | 0.02 | 1.51 |
| 385.90 | 83.77 | 0.19 | 3.62 | 2.13 | 0.07 | 0.63 | 5.08 | 0.60 | 0.74 | 0.03 | 3.14 |
| 390.75 | 86.11 | 0.19 | 3.78 | 3.32 | 0.05 | 2.81 | 0.59 | 0.73 | 1.00 | 0.02 | 1.39 |
| 392.54 | 71.12 | 0.22 | 3.70 | 3.90 | 0.11 | 3.73 | 9.30 | 0.80 | 0.81 | 0.03 | 6.27 |
| 396.55 | 79.98 | 0.18 | 2.77 | 2.24 | 0.08 | 1.17 | 7.91 | 0.47 | 0.70 | 0.04 | 4.47 |
| 401.51 | 85.62 | 0.17 | 3.96 | 2.71 | 0.05 | 2.80 | 1.08 | 0.74 | 0.98 | 0.03 | 1.87 |
| 405.70 | 73.45 | 0.36 | 6.34 | 3.97 | 0.08 | 5.32 | 3.92 | 1.23 | 1.81 | 0.03 | 3.49 |
| 412.50 | 79.11 | 0.32 | 5.95 | 2.95 | 0.06 | 4.63 | 1.51 | 1.16 | 1.77 | 0.04 | 2.50 |
| 413.06 | 81.85 | 0.29 | 5.18 | 2.99 | 0.06 | 4.40 | 1.05 | 1.11 | 1.47 | 0.03 | 1.58 |
| 419.00 | 71.68 | 0.09 | 1.29 | 1.81 | 0.15 | 0.98 | 13.53 | 0.33 | 0.21 | 0.07 | 9.87 |
| 422.78 | 80.87 | 0.12 | 1.41 | 1.68 | 0.10 | 1.34 | 9.41 | 0.24 | 0.38 | 0.02 | 4.43 |
| 426.13 | 92.45 | 0.10 | 2.17 | 1.37 | 0.05 | 1.60 | 0.52 | 0.36 | 0.67 | 0.02 | 0.67 |
| 426.74 | 87.30 | 0.11 | 2.11 | 1.39 | 0.06 | 1.32 | 3.66 | 0.46 | 0.68 | 0.02 | 2.88 |
| 432.02 | 86.01 | 0.16 | 3.31 | 2.27 | 0.06 | 4.09 | 1.12 | 0.71 | 1.04 | 0.02 | 1.20 |
| 437.09 | 78.67 | 0.27 | 5.83 | 3.32 | 0.06 | 6.69 | 0.50 | 1.08 | 2.34 | 0.03 | 1.20 |
| 440.24 | 80.64 | 0.28 | 4.76 | 3.88 | 0.07 | 5.06 | 0.79 | 1.10 | 1.67 | 0.04 | 1.72 |
| 445.20 | 93.07 | 0.09 | 1.38 | 0.63 | 0.06 | 0.27 | 2.21 | 0.21 | 0.28 | 0.02 | 1.78 |
| 449.70 | 63.84 | 0.07 | 0.90 | 0.59 | 0.19 | 0.27 | 21.84 | 0.16 | 0.20 | 0.03 | 11.90 |
| 450.21 | 91.38 | 0.08 | 1.27 | 1.19 | 0.07 | 0.32 | 2.78 | 0.20 | 0.29 | 0.01 | 2.42 |
| 455.84 | 85.67 | 0.19 | 4.23 | 2.34 | 0.07 | 1.33 | 1.94 | 0.64 | 1.07 | 0.03 | 2.50 |
| 460.10 | 82.60 | 0.19 | 3.55 | 2.01 | 0.07 | 2.99 | 3.51 | 0.65 | 1.30 | 0.02 | 3.10 |
| 466.34 | 89.09 | 0.17 | 2.73 | 1.79 | 0.06 | 2.33 | 1.12 | 0.56 | 0.96 | 0.02 | 1.17 |
| 473.58 | 88.03 | 0.12 | 3.01 | 2.30 | 0.06 | 3.05 | 0.46 | 0.63 | 0.78 | 0.02 | 1.55 |
| 475.31 | 85.81 | 0.17 | 3.96 | 2.18 | 0.06 | 3.07 | 0.60 | 0.75 | 1.47 | 0.04 | 1.89 |
| 480.63 | 79.28 | 0.25 | 4.58 | 3.82 | 0.08 | 2.55 | 4.05 | 0.82 | 1.47 | 0.04 | 3.07 |
| 481.19 | 86.41 | 0.18 | 3.04 | 2.90 | 0.07 | 2.15 | 2.18 | 0.52 | 0.65 | 0.02 | 1.87 |
| 486.00 | 92.69 | 0.11 | 1.71 | 1.13 | 0.06 | 0.33 | 1.62 | 0.17 | 0.42 | 0.02 | 1.73 |
| 490.91 | 90.70 | 0.09 | 1.48 | 1.35 | 0.07 | 0.39 | 2.86 | 0.23 | 0.37 | 0.02 | 2.43 |
| 495.12 | 96.35 | 0.05 | 0.90 | 0.55 | 0.05 | 0.25 | 0.51 | 0.13 | 0.24 | 0.00 | 0.96 |
| 500.18 | 98.67 | 0.04 | 0.43 | 0.17 | 0.05 | 0.15 | 0.05 | 0.09 | 0.14 | 0.01 | 0.20 |
| 505.30 | 97.08 | 0.04 | 0.65 | 0.28 | 0.05 | 0.23 | 0.62 | 0.12 | 0.18 | 0.01 | 0.73 |
| 509.33 | 85.61 | 0.12 | 2.03 | 1.99 | 0.09 | 0.39 | 4.95 | 0.23 | 0.65 | 0.02 | 3.92 |
| 513.14 | 91.33 | 0.11 | 1.85 | 0.97 | 0.07 | 0.31 | 2.75 | 0.24 | 0.66 | 0.02 | 1.68 |
| 518.97 | 80.33 | 0.14 | 2.75 | 2.37 | 0.08 | 0.56 | 7.32 | 0.40 | 0.72 | 0.02 | 5.31 |
| 525.33 | 83.59 | 0.08 | 1.71 | 1.15 | 0.07 | 0.37 | 7.26 | 0.16 | 0.31 | 0.01 | 5.30 |
| 531.78 | 95.63 | 0.06 | 0.81 | 0.64 | 0.05 | 0.28 | 0.90 | 0.13 | 0.23 | 0.01 | 1.25 |
| 533.19 | 88.98 | 0.07 | 1.58 | 1.32 | 0.07 | 0.33 | 3.70 | 0.15 | 0.45 | 0.01 | 3.34 |
| 540.07 | 84.51 | 0.22 | 3.17 | 3.23 | 0.07 | 3.23 | 2.22 | 0.70 | 0.89 | 0.03 | 1.74 |
| 543.82 | 82.26 | 0.21 | 3.72 | 3.58 | 0.06 | 6.12 | 0.51 | 1.17 | 0.99 | 0.02 | 1.35 |
| 546.10 | 86.90 | 0.16 | 2.89 | 2.63 | 0.06 | 4.10 | 0.84 | 0.77 | 0.76 | 0.02 | 0.87 |
| 550.00 | 81.49 | 0.18 | 3.64 | 3.37 | 0.06 | 5.39 | 1.59 | 0.95 | 0.85 | 0.02 | 2.45 |
| 556.17 | 82.50 | 0.29 | 4.78 | 3.69 | 0.06 | 4.09 | 1.07 | 1.12 | 1.04 | 0.02 | 1.33 |
| 560.89 | 93.66 | 0.13 | 2.61 | 0.76 | 0.05 | 0.43 | 0.69 | 0.44 | 0.60 | 0.01 | 0.60 |
| 566.07 | 96.41 | 0.09 | 1.44 | 0.39 | 0.05 | 0.01 | 0.13 | 0.20 | 0.41 | 0.01 | 0.85 |
| 577.10 | 70.88 | 0.12 | 1.47 | 1.98 | 0.14 | 0.28 | 13.04 | 0.24 | 0.33 | 0.03 | 11.47 |
| 581.97 | 71.66 | 0.52 | 9.36 | 6.47 | 0.10 | 3.34 | 3.25 | 1.21 | 1.54 | 0.06 | 2.50 |
| 586.78 | 90.03 | 0.18 | 2.62 | 1.94 | 0.05 | 1.42 | 1.32 | 0.46 | 0.59 | 0.02 | 1.37 |
| 586.78 | 90.02 | 0.18 | 2.58 | 1.95 | 0.05 | 1.44 | 1.33 | 0.47 | 0.59 | 0.02 | 1.37 |
| 594.21 | 84.20 | 0.16 | 3.38 | 2.82 | 0.06 | 1.88 | 3.20 | 0.64 | 0.92 | 0.02 | 2.71 |
| 602.09 | 87.63 | 0.17 | 4.42 | 1.58 | 0.05 | 1.94 | 0.56 | 0.80 | 1.33 | 0.02 | 1.51 |
| 606.51 | 86.81 | 0.08 | 1.79 | 1.91 | 0.07 | 1.87 | 3.15 | 0.21 | 0.53 | 0.01 | 3.57 |
| 613.25 | 74.57 | 0.16 | 3.30 | 3.26 | 0.08 | 1.60 | 8.83 | 0.57 | 0.79 | 0.03 | 6.82 |
| 615.34 | 66.55 | 0.64 | 12.99 | 5.99 | 0.08 | 3.17 | 3.44 | 1.42 | 2.36 | 0.12 | 3.23 |
| 620.43 | 83.43 | 0.20 | 4.96 | 2.38 | 0.06 | 2.43 | 2.19 | 1.03 | 1.13 | 0.03 | 2.16 |
| 626.15 | 81.25 | 0.11 | 2.34 | 1.67 | 0.07 | 1.17 | 7.33 | 0.40 | 0.63 | 0.02 | 5.00 |
| 630.35 | 85.12 | 0.17 | 2.91 | 2.76 | 0.07 | 3.50 | 2.34 | 0.67 | 0.54 | 0.02 | 1.91 |
| 634.73 | 81.34 | 0.23 | 4.28 | 3.88 | 0.06 | 5.67 | 1.12 | 1.21 | 0.69 | 0.02 | 1.49 |
| 638.27 | 81.47 | 0.22 | 5.27 | 3.17 | 0.06 | 5.60 | 1.31 | 1.36 | 0.92 | 0.03 | 0.59 |
| 643.08 | 82.26 | 0.21 | 3.56 | 3.80 | 0.06 | 6.21 | 0.77 | 1.04 | 0.53 | 0.02 | 1.55 |
| 649.11 | 76.02 | 0.27 | 5.06 | 4.58 | 0.06 | 8.69 | 1.22 | 1.44 | 0.74 | 0.03 | 1.90 |
| 655.83 | 73.68 | 0.31 | 6.70 | 5.17 | 0.07 | 8.83 | 0.81 | 1.56 | 1.04 | 0.03 | 1.80 |
| 659.10 | 76.12 | 0.24 | 7.23 | 4.01 | 0.07 | 7.37 | 0.70 | 1.67 | 1.12 | 0.02 | 1.44 |
| 664.00 | 84.76 | 0.22 | 5.56 | 2.04 | 0.06 | 2.99 | 0.67 | 1.05 | 1.11 | 0.02 | 1.52 |

Tab. 1 - Continued.

| Depth | SiO ₂ | TiO ₂ | Al ₂ O ₃ | Fe ₂ O ₃ | MnO | MgO | CaO | Na ₂ O | K ₂ O | P ₂ O ₅ | L.O.I |
|--------|------------------|------------------|--------------------------------|--------------------------------|------|-------|------|-------------------|------------------|-------------------------------|-------|
| 669.63 | 87.06 | 0.17 | 3.31 | 3.02 | 0.06 | 3.93 | 0.47 | 0.80 | 0.80 | 0.02 | 0.37 |
| 673.25 | 76.76 | 0.22 | 5.04 | 4.83 | 0.07 | 8.47 | 1.00 | 1.54 | 0.59 | 0.02 | 1.46 |
| 676.29 | 75.97 | 0.38 | 8.37 | 3.84 | 0.06 | 4.81 | 0.94 | 1.46 | 1.42 | 0.04 | 2.71 |
| 680.99 | 79.04 | 0.23 | 4.95 | 4.37 | 0.06 | 6.79 | 1.01 | 1.27 | 0.79 | 0.03 | 1.45 |
| 685.33 | 83.89 | 0.19 | 3.73 | 3.15 | 0.06 | 5.32 | 0.72 | 0.97 | 0.64 | 0.02 | 1.31 |
| 686.49 | 81.80 | 0.18 | 4.20 | 3.20 | 0.06 | 6.58 | 0.70 | 1.07 | 0.93 | 0.02 | 1.25 |
| 691.11 | 78.11 | 0.25 | 4.81 | 4.87 | 0.07 | 7.78 | 1.14 | 1.29 | 0.65 | 0.03 | 0.98 |
| 696.37 | 66.34 | 0.37 | 8.35 | 6.30 | 0.08 | 11.50 | 1.96 | 1.89 | 1.12 | 0.03 | 2.06 |
| 696.74 | 72.38 | 0.31 | 7.78 | 4.53 | 0.07 | 8.78 | 1.67 | 1.80 | 1.19 | 0.04 | 1.44 |
| 704.84 | 74.12 | 0.29 | 7.36 | 4.27 | 0.07 | 7.81 | 1.41 | 1.73 | 1.22 | 0.03 | 1.69 |
| 708.45 | 75.18 | 0.31 | 6.71 | 4.68 | 0.07 | 7.55 | 1.41 | 1.69 | 0.89 | 0.03 | 1.48 |
| 710.63 | 74.33 | 0.34 | 7.13 | 5.78 | 0.07 | 6.53 | 1.25 | 1.31 | 1.05 | 0.03 | 2.18 |
| 715.50 | 77.43 | 0.29 | 4.73 | 5.12 | 0.08 | 7.24 | 1.40 | 1.31 | 0.65 | 0.03 | 1.73 |
| 720.87 | 71.82 | 0.32 | 7.31 | 5.43 | 0.07 | 9.16 | 2.02 | 1.78 | 0.93 | 0.03 | 1.12 |
| 724.05 | 76.90 | 0.24 | 5.37 | 4.63 | 0.07 | 7.91 | 1.37 | 1.36 | 0.73 | 0.03 | 1.38 |
| 730.84 | 73.98 | 0.32 | 6.30 | 4.98 | 0.08 | 8.93 | 1.20 | 1.50 | 1.07 | 0.03 | 1.60 |
| 735.36 | 74.28 | 0.29 | 6.34 | 4.92 | 0.07 | 8.50 | 1.41 | 1.42 | 0.93 | 0.02 | 1.81 |
| 737.32 | 72.03 | 0.32 | 6.55 | 4.97 | 0.08 | 9.21 | 1.93 | 1.48 | 0.86 | 0.03 | 2.54 |
| 740.86 | 79.50 | 0.29 | 4.56 | 4.82 | 0.07 | 6.46 | 1.18 | 1.20 | 0.60 | 0.05 | 1.29 |
| 744.85 | 75.92 | 0.29 | 6.74 | 3.83 | 0.07 | 7.30 | 1.50 | 1.69 | 1.06 | 0.04 | 1.56 |
| 750.04 | 74.88 | 0.33 | 7.54 | 3.58 | 0.07 | 7.08 | 1.44 | 1.60 | 1.40 | 0.03 | 2.05 |
| 754.84 | 77.83 | 0.23 | 5.87 | 3.73 | 0.06 | 6.14 | 1.25 | 1.37 | 0.88 | 0.03 | 2.60 |
| 759.71 | 71.86 | 0.33 | 8.12 | 4.79 | 0.07 | 7.43 | 1.49 | 1.56 | 1.27 | 0.03 | 3.05 |
| 765.03 | 73.55 | 0.56 | 6.98 | 5.14 | 0.07 | 7.68 | 1.32 | 1.50 | 1.26 | 0.03 | 1.90 |
| 770.23 | 71.16 | 0.35 | 7.47 | 5.03 | 0.07 | 7.21 | 2.25 | 1.50 | 1.04 | 0.03 | 3.89 |
| 776.58 | 85.30 | 0.29 | 3.57 | 3.31 | 0.06 | 3.32 | 1.25 | 0.68 | 0.63 | 0.03 | 1.56 |
| 777.67 | 79.37 | 0.31 | 5.35 | 4.12 | 0.07 | 4.64 | 2.48 | 1.00 | 0.97 | 0.04 | 1.64 |
| 780.51 | 84.44 | 0.12 | 2.19 | 1.39 | 0.09 | 1.47 | 5.35 | 0.37 | 0.50 | 0.02 | 4.05 |
| 787.68 | 72.66 | 0.31 | 6.95 | 5.75 | 0.07 | 7.45 | 1.72 | 1.44 | 1.44 | 0.05 | 2.14 |

SiO₂ values in the interval between approximately 200 and 600 mbsf account for increased proportions of quartz grains suggested on the basis of sand grain compositional modes (Cape Roberts Science Team, 2000).

Ni and Cr curves closely mirror the SiO₂ profile (Fig. 1). Above 160 mbsf and below 600 mbsf, values mainly fluctuate between 20 and 40 ppm and between 30 and 60 ppm for Ni and Cr, respectively. Concentrations of these elements are markedly lower through the interval between 160 and 600 mbsf. Given that modal investigations in CRP-3 have revealed the absence of alkaline volcanic lithic grains and ferromagnesian minerals typical of the McMurdo Volcanic Group (Smellie, this volume), the higher contents of Ni and Cr in the sediments above 160 mbsf and below 600 mbsf should be derived from the Ferrar dolerite. These elements average 61 and 96 ppm in the Ferrar dolerite, whereas they are very depleted (6 and 18 ppm) in the Beacon Sandstone (Roser & Pyne, 1989).

The vanadium profile (Fig. 1) is similar to those of Ni and Cr and supports the suggestion of an influence of Ferrar detritus in the upper and lower part of the CRP-3 core and a dominant input of Beacon materials in the rest of the drillhole. In fact, V is typically enriched in the Ferrar dolerite (283 ppm) and depleted in the Lower Beacon (25 ppm; Roser & Pyne, 1989).

Also Rb/Sr ratios, that are lower (on average 0.42) above approximately 200 and below 600 mbsf

(Fig. 2) are compatible with a dominant Ferrar (Rb/Sr=0.34) provenance of the detritus in these stratigraphic intervals. Throughout the rest of the drillhole, the Rb/Sr ratios widely fluctuate with averagely higher values (0.88) reflecting a striking influence of the Beacon sandstone (Rb/Sr=1.17; Roser & Pyne, 1989).

Our suggestions on the sediment provenance based on geochemical proxies from the CRP-3 drillhole are consistent with the results from sandstone detrital modes (Smellie, this volume) and clay mineral assemblages (Ehrmann, this volume).

Concentrations of zirconium (Fig. 2) exhibit high variability in CRP-3 sediments and the stratigraphic profile of this element does not correlate with those of SiO₂, Ni, Cr, V, and Rb/Sr. A reason for this could be the similar contents of Zr in the two main sources, Beacon and Ferrar (142 ppm for both sources; Roser & Pyne, 1989).

Ca values in CRP-3 (Fig. 2) are mostly about 2% but many anomalously high concentrations, measured between 200 and 600 mbsf, reveal the occurrence of diagenetic carbonate.

SPECTRAL ANALYSIS AND TIME FRAMEWORK

An ensemble of geochemical signals obtained from the CRP-3 core were processed by spectral analysis. The original adopted sampling rate (on average 1 sample/5 m) did not allow us to extract from the geochemical signals of the upper part of the

Tab. 2 - Trace element concentrations (ppm) of CRP-3 samples.

| Depth (mbsf) | Rb | Sr | Zr | Cr | V | Ni | Ba | La | Ce | Y | Nb | Rb/Sr |
|--------------|----|-----|-----|-----|-----|----|-----|----|----|----|----|-------|
| 5.77 | 47 | 74 | 72 | 43 | 96 | 20 | 328 | 19 | 32 | 0 | 15 | 0.626 |
| 9.90 | 40 | 76 | 76 | 45 | 102 | 21 | 324 | 21 | 46 | 0 | 16 | 0.523 |
| 13.26 | 49 | 76 | 83 | 53 | 112 | 21 | 361 | 21 | 37 | 0 | 17 | 0.644 |
| 21.16 | 40 | 75 | 146 | 36 | 97 | 22 | 268 | 10 | 15 | 22 | 13 | 0.527 |
| 24.32 | 44 | 85 | 212 | 37 | 91 | 20 | 246 | 13 | 24 | 22 | 13 | 0.525 |
| 24.88 | 18 | 39 | 107 | 24 | 57 | 14 | 150 | 6 | 11 | 10 | 8 | 0.461 |
| 28.80 | 34 | 63 | 139 | 34 | 88 | 19 | 232 | 13 | 22 | 19 | 12 | 0.529 |
| 33.14 | 50 | 83 | 164 | 47 | 112 | 23 | 317 | 16 | 24 | 35 | 15 | 0.594 |
| 47.61 | 63 | 123 | 154 | 52 | 124 | 33 | 379 | 26 | 60 | 0 | 19 | 0.510 |
| 49.40 | 60 | 90 | 144 | 59 | 130 | 29 | 373 | 30 | 57 | 0 | 17 | 0.663 |
| 67.03 | 27 | 61 | 94 | 25 | 65 | 18 | 176 | 15 | 20 | 11 | 10 | 0.447 |
| 69.97 | 52 | 95 | 136 | 47 | 115 | 23 | 318 | 27 | 29 | 31 | 13 | 0.553 |
| 73.40 | 44 | 71 | 37 | 59 | 142 | 34 | 377 | 24 | 59 | 11 | 17 | 0.625 |
| 78.35 | 70 | 136 | 193 | 58 | 141 | 36 | 381 | 16 | 34 | 31 | 15 | 0.518 |
| 83.39 | 51 | 124 | 168 | 52 | 115 | 34 | 353 | 18 | 45 | 24 | 12 | 0.414 |
| 89.47 | 55 | 140 | 154 | 57 | 121 | 32 | 371 | 21 | 56 | 3 | 13 | 0.390 |
| 94.47 | 36 | 189 | 217 | 38 | 98 | 21 | 230 | 14 | 30 | 26 | 11 | 0.188 |
| 99.47 | 85 | 244 | 231 | 52 | 121 | 32 | 391 | 20 | 40 | 37 | 15 | 0.346 |
| 103.58 | 73 | 207 | 178 | 49 | 115 | 27 | 393 | 25 | 53 | 31 | 13 | 0.353 |
| 110.16 | 76 | 241 | 144 | 51 | 115 | 27 | 408 | 27 | 63 | 33 | 14 | 0.315 |
| 115.87 | 56 | 161 | 185 | 42 | 96 | 22 | 340 | 15 | 39 | 24 | 13 | 0.345 |
| 123.42 | 69 | 198 | 70 | 58 | 122 | 31 | 451 | 36 | 69 | 0 | 18 | 0.348 |
| 130.57 | 95 | 257 | 212 | 56 | 131 | 26 | 370 | 24 | 44 | 27 | 13 | 0.371 |
| 135.15 | 70 | 208 | 146 | 52 | 133 | 30 | 363 | 23 | 43 | 36 | 15 | 0.335 |
| 139.88 | 19 | 259 | 192 | 36 | 75 | 20 | 532 | 11 | 4 | 27 | 8 | 0.075 |
| 145.09 | 28 | 122 | 202 | 39 | 124 | 27 | 177 | 2 | 11 | 21 | 9 | 0.226 |
| 148.73 | 24 | 123 | 240 | 40 | 110 | 23 | 155 | 3 | 3 | 18 | 10 | 0.199 |
| 155.82 | 22 | 120 | 186 | 25 | 57 | 13 | 152 | 8 | 4 | 13 | 10 | 0.185 |
| 156.52 | 24 | 186 | 84 | 28 | 69 | 16 | 185 | 7 | 7 | 0 | 10 | 0.132 |
| 168.94 | 61 | 171 | 205 | 37 | 120 | 23 | 321 | 14 | 29 | 25 | 13 | 0.359 |
| 171.75 | 8 | 12 | 70 | 6 | 14 | 4 | 63 | 2 | 0 | 7 | 8 | 0.690 |
| 171.95 | 50 | 152 | 219 | 40 | 106 | 22 | 252 | 18 | 28 | 22 | 13 | 0.326 |
| 177.19 | 38 | 320 | 146 | 22 | 60 | 17 | 211 | 14 | 15 | 27 | 7 | 0.120 |
| 177.47 | 50 | 123 | 279 | 35 | 72 | 17 | 254 | 13 | 17 | 24 | 12 | 0.410 |
| 183.66 | 8 | 77 | 17 | 13 | 45 | 11 | 145 | 4 | 1 | 7 | 14 | 0.102 |
| 189.16 | 99 | 226 | 155 | 44 | 95 | 24 | 351 | 36 | 55 | 50 | 13 | 0.439 |
| 189.51 | 31 | 319 | 85 | 25 | 54 | 13 | 165 | 8 | 6 | 8 | 7 | 0.097 |
| 196.27 | 74 | 202 | 177 | 41 | 96 | 21 | 326 | 18 | 30 | 26 | 15 | 0.369 |
| 202.56 | 20 | 104 | 74 | 21 | 44 | 13 | 184 | 6 | 0 | 0 | 11 | 0.187 |
| 207.68 | 34 | 45 | 98 | 34 | 91 | 20 | 207 | 7 | 18 | 0 | 14 | 0.744 |
| 210.49 | 49 | 81 | 275 | 33 | 77 | 17 | 224 | 11 | 13 | 29 | 11 | 0.605 |
| 215.39 | 19 | 82 | 166 | 34 | 84 | 17 | 134 | 7 | 18 | 0 | 13 | 0.235 |
| 226.39 | 30 | 37 | 121 | 22 | 71 | 15 | 135 | 5 | 0 | 13 | 10 | 0.790 |
| 229.00 | 92 | 69 | 177 | 44 | 119 | 31 | 348 | 14 | 32 | 18 | 13 | 1.331 |
| 230.42 | 29 | 136 | 149 | 41 | 63 | 19 | 194 | 12 | 3 | 25 | 11 | 0.215 |
| 235.47 | 22 | 94 | 123 | 29 | 50 | 15 | 405 | 6 | 4 | 23 | 8 | 0.235 |
| 239.86 | 35 | 34 | 104 | 30 | 78 | 17 | 171 | 6 | 0 | 35 | 11 | 1.030 |
| 244.83 | 20 | 32 | 117 | 18 | 54 | 11 | 118 | 0 | 0 | 10 | 10 | 0.620 |
| 250.24 | 23 | 30 | 161 | 23 | 58 | 10 | 117 | 3 | 6 | 14 | 9 | 0.780 |
| 256.63 | 63 | 68 | 291 | 29 | 68 | 14 | 212 | 4 | 9 | 15 | 11 | 0.924 |
| 259.30 | 56 | 47 | 161 | 27 | 66 | 16 | 222 | 9 | 10 | 15 | 12 | 1.191 |
| 270.94 | 14 | 51 | 81 | 14 | 39 | 10 | 138 | 2 | 0 | 16 | 9 | 0.269 |
| 273.85 | 39 | 89 | 149 | 22 | 55 | 11 | 177 | 8 | 4 | 16 | 10 | 0.439 |
| 279.65 | 40 | 87 | 228 | 42 | 88 | 17 | 180 | 7 | 10 | 14 | 9 | 0.452 |
| 283.21 | 24 | 93 | 70 | 48 | 117 | 19 | 412 | 7 | 2 | 0 | 14 | 0.263 |
| 286.19 | 51 | 87 | 178 | 47 | 117 | 25 | 213 | 4 | 7 | 9 | 10 | 0.589 |
| 289.17 | 18 | 43 | 163 | 23 | 65 | 15 | 123 | 5 | 2 | 16 | 9 | 0.419 |
| 291.40 | 21 | 45 | 178 | 54 | 152 | 20 | 136 | 3 | 12 | 47 | 12 | 0.472 |
| 298.96 | 19 | 38 | 81 | 27 | 80 | 16 | 132 | 7 | 13 | 4 | 12 | 0.489 |
| 301.64 | 22 | 29 | 91 | 24 | 100 | 11 | 144 | 4 | 1 | 0 | 13 | 0.743 |
| 305.71 | 32 | 39 | 135 | 21 | 64 | 7 | 144 | 2 | 0 | 9 | 9 | 0.817 |
| 312.35 | 92 | 62 | 200 | 38 | 100 | 20 | 281 | 9 | 12 | 18 | 11 | 1.476 |
| 315.74 | 94 | 70 | 181 | 46 | 126 | 25 | 324 | 21 | 37 | 23 | 14 | 1.339 |
| 320.60 | 77 | 53 | 72 | 50 | 134 | 30 | 390 | 20 | 48 | 0 | 18 | 1.460 |
| 326.64 | 17 | 14 | 18 | 16 | 33 | 8 | 126 | 2 | 0 | 6 | 12 | 1.169 |
| 333.16 | 21 | 48 | 132 | 16 | 57 | 16 | 174 | 5 | 2 | 23 | 11 | 0.439 |
| 335.93 | 28 | 43 | 257 | 24 | 58 | 12 | 126 | 3 | 1 | 15 | 10 | 0.646 |
| 341.11 | 62 | 55 | 211 | 31 | 73 | 18 | 208 | 7 | 4 | 22 | 11 | 1.123 |
| 345.73 | 15 | 36 | 46 | 29 | 79 | 13 | 158 | 9 | 0 | 8 | 14 | 0.414 |
| 348.67 | 9 | 17 | 47 | 11 | 31 | 9 | 108 | 7 | 0 | 0 | 13 | 0.531 |
| 351.85 | 29 | 89 | 105 | 45 | 108 | 23 | 281 | 12 | 9 | 8 | 8 | 0.330 |
| 356.15 | 63 | 80 | 131 | 33 | 68 | 17 | 245 | 4 | 11 | 10 | 9 | 0.796 |
| 358.92 | 56 | 54 | 152 | 35 | 83 | 25 | 199 | 2 | 11 | 11 | 9 | 1.038 |
| 365.84 | 25 | 32 | 179 | 23 | 36 | 11 | 132 | 3 | 8 | 16 | 10 | 0.786 |
| 369.61 | 12 | 28 | 108 | 18 | 38 | 10 | 96 | 5 | 12 | 18 | 10 | 0.441 |
| 375.29 | 12 | 26 | 80 | 29 | 53 | 23 | 99 | 7 | 0 | 13 | 9 | 0.457 |
| 381.97 | 18 | 24 | 90 | 36 | 79 | 12 | 123 | 9 | 0 | 0 | 11 | 0.758 |
| 385.90 | 24 | 41 | 110 | 37 | 73 | 14 | 137 | 5 | 10 | 12 | 9 | 0.583 |
| 390.75 | 39 | 41 | 142 | 39 | 84 | 17 | 158 | 3 | 0 | 10 | 10 | 0.964 |
| 392.54 | 33 | 46 | 83 | 41 | 91 | 25 | 152 | 14 | 24 | 44 | 10 | 0.719 |
| 396.55 | 22 | 32 | 102 | 29 | 58 | 19 | 118 | 5 | 1 | 18 | 10 | 0.697 |
| 401.51 | 33 | 40 | 101 | 31 | 76 | 17 | 160 | 6 | 7 | 14 | 9 | 0.817 |
| 405.70 | 91 | 68 | 195 | 39 | 119 | 28 | 264 | 9 | 10 | 15 | 10 | 1.343 |
| 412.50 | 83 | 66 | 277 | 34 | 87 | 19 | 246 | 5 | 7 | 18 | 12 | 1.248 |
| 413.06 | 58 | 51 | 194 | 29 | 84 | 17 | 219 | 9 | 15 | 19 | 14 | 1.142 |
| 419.00 | 3 | 42 | 45 | 371 | 30 | 11 | 80 | 4 | 0 | 0 | 11 | 0.082 |

Tab. 2 - Continued.

| Depth (mbsf) | Rb | Sr | Zr | Cr | V | Ni | Ba | La | Ce | Y | Nb | Rb/Sr |
|--------------|-----|-----|-----|-----|-----|----|-----|----|----|----|----|-------|
| 422.78 | 8 | 17 | 141 | 27 | 52 | 18 | 82 | 6 | 3 | 30 | 10 | 0.470 |
| 426.13 | 23 | 22 | 98 | 17 | 40 | 10 | 113 | 7 | 0 | 9 | 9 | 1.056 |
| 426.74 | 20 | 18 | 72 | 18 | 42 | 11 | 108 | 5 | 0 | 37 | 11 | 1.102 |
| 432.02 | 38 | 24 | 128 | 27 | 73 | 20 | 140 | 3 | 0 | 14 | 10 | 1.603 |
| 437.09 | 102 | 44 | 246 | 35 | 104 | 21 | 210 | 8 | 5 | 9 | 11 | 2.330 |
| 440.24 | 66 | 34 | 176 | 36 | 99 | 20 | 191 | 5 | 8 | 30 | 12 | 1.951 |
| 445.20 | 9 | 19 | 98 | 17 | 34 | 8 | 73 | 0 | -8 | 13 | 8 | 0.465 |
| 449.70 | 9 | 34 | 65 | 21 | 25 | 8 | 59 | 0 | 3 | 24 | 8 | 0.254 |
| 450.21 | 9 | 18 | 64 | 13 | 28 | 9 | 91 | 1 | 2 | 10 | 10 | 0.494 |
| 455.84 | 28 | 29 | 85 | 27 | 64 | 16 | 154 | 2 | 10 | 0 | 11 | 0.973 |
| 460.10 | 55 | 37 | 171 | 27 | 63 | 17 | 177 | 7 | 9 | 11 | 9 | 1.511 |
| 466.34 | 33 | 26 | 154 | 21 | 50 | 11 | 148 | 3 | 3 | 21 | 9 | 1.270 |
| 473.58 | 25 | 21 | 119 | 11 | 43 | 10 | 102 | 13 | 8 | 10 | 10 | 1.167 |
| 475.31 | 64 | 41 | 204 | 25 | 66 | 22 | 209 | 5 | 0 | 10 | 10 | 1.575 |
| 480.63 | 69 | 37 | 116 | 47 | 100 | 39 | 172 | 9 | 7 | 12 | 9 | 1.847 |
| 481.19 | 22 | 18 | 116 | 24 | 77 | 26 | 100 | 5 | -8 | 22 | 12 | 1.198 |
| 486.00 | 12 | 9 | 70 | 15 | 37 | 10 | 74 | 6 | 0 | 12 | 9 | 1.258 |
| 490.91 | 13 | 15 | 86 | 17 | 35 | 7 | 81 | 7 | 3 | 11 | 9 | 0.875 |
| 495.12 | 7 | 6 | 70 | 6 | 17 | 4 | 57 | 1 | 0 | 3 | 11 | 1.161 |
| 500.18 | 6 | 6 | 55 | 4 | 8 | 2 | 39 | 0 | 0 | 6 | 8 | 0.878 |
| 505.30 | 6 | 9 | 62 | 7 | 12 | 3 | 49 | 2 | 0 | 7 | 8 | 0.729 |
| 509.33 | 25 | 22 | 152 | 20 | 37 | 9 | 107 | 6 | 3 | 9 | 9 | 1.143 |
| 513.14 | 18 | 12 | 74 | 16 | 30 | 24 | 93 | 3 | 5 | 0 | 11 | 1.583 |
| 518.97 | 25 | 29 | 114 | 30 | 52 | 12 | 132 | 5 | 1 | 23 | 11 | 0.876 |
| 525.33 | 16 | 27 | 76 | 17 | 45 | 8 | 61 | 2 | 2 | 6 | 8 | 0.582 |
| 531.78 | 7 | 7 | 71 | 12 | 19 | 5 | 61 | 3 | 6 | 9 | 9 | 1.013 |
| 533.19 | 12 | 11 | 47 | 11 | 21 | 7 | 84 | 1 | -9 | 9 | 9 | 1.073 |
| 540.07 | 39 | 31 | 121 | 45 | 100 | 25 | 110 | 2 | 0 | 15 | 9 | 1.260 |
| 543.82 | 34 | 26 | 114 | 59 | 104 | 26 | 141 | 1 | 4 | 27 | 11 | 1.302 |
| 546.10 | 23 | 22 | 94 | 38 | 73 | 23 | 118 | 4 | 3 | 0 | 12 | 1.064 |
| 550.00 | 30 | 34 | 117 | 47 | 93 | 30 | 154 | 6 | 2 | 29 | 11 | 0.875 |
| 556.17 | 28 | 39 | 107 | 65 | 133 | 33 | 172 | 0 | 0 | 0 | 12 | 0.708 |
| 560.89 | 17 | 24 | 99 | 20 | 45 | 7 | 110 | 3 | 0 | 5 | 11 | 0.732 |
| 566.07 | 15 | 12 | 77 | 13 | 23 | 11 | 155 | 1 | 0 | 12 | 9 | 1.325 |
| 577.10 | 6 | 31 | 100 | 383 | 33 | 10 | 83 | 3 | 0 | 0 | 13 | 0.184 |
| 581.97 | 54 | 67 | 104 | 114 | 193 | 46 | 317 | 5 | 14 | 16 | 11 | 0.796 |
| 586.78 | 25 | 29 | 134 | 32 | 70 | 17 | 114 | 8 | 0 | 12 | 9 | 0.863 |
| 594.21 | 31 | 39 | 87 | 29 | 69 | 13 | 160 | 5 | 0 | 15 | 12 | 0.803 |
| 602.09 | 44 | 37 | 120 | 26 | 66 | 23 | 206 | 6 | 1 | 18 | 10 | 1.174 |
| 606.51 | 12 | 26 | 68 | 13 | 26 | 6 | 83 | 0 | 7 | 9 | 12 | 0.471 |
| 613.25 | 35 | 63 | 155 | 33 | 61 | 15 | 170 | 4 | 12 | 13 | 8 | 0.551 |
| 615.34 | 39 | 54 | 160 | 29 | 63 | 30 | 177 | 11 | 14 | 14 | 9 | 0.724 |
| 620.43 | 48 | 69 | 152 | 34 | 84 | 20 | 205 | 8 | 10 | 12 | 9 | 0.687 |
| 626.15 | 23 | 49 | 111 | 18 | 36 | 13 | 122 | 3 | 0 | 15 | 9 | 0.478 |
| 630.35 | 13 | 33 | 96 | 38 | 76 | 22 | 136 | 2 | 0 | 0 | 12 | 0.412 |
| 634.73 | 20 | 48 | 143 | 55 | 117 | 32 | 161 | 4 | 13 | 13 | 10 | 0.415 |
| 638.27 | 29 | 60 | 142 | 40 | 95 | 24 | 196 | 9 | 5 | 16 | 10 | 0.480 |
| 643.08 | 20 | 45 | 169 | 52 | 109 | 31 | 136 | 4 | 7 | 16 | 9 | 0.441 |
| 649.11 | 31 | 67 | 181 | 84 | 146 | 44 | 181 | 7 | 5 | 21 | 10 | 0.455 |
| 655.83 | 31 | 59 | 156 | 91 | 165 | 43 | 180 | 10 | 0 | 9 | 12 | 0.515 |
| 659.10 | 46 | 83 | 170 | 54 | 111 | 31 | 204 | 7 | 10 | 15 | 10 | 0.554 |
| 664.00 | 35 | 68 | 140 | 36 | 72 | 22 | 206 | 10 | 8 | 28 | 11 | 0.517 |
| 669.63 | 16 | 30 | 137 | 45 | 85 | 27 | 132 | 5 | 0 | 27 | 11 | 0.525 |
| 673.25 | 18 | 50 | 115 | 58 | 131 | 33 | 123 | 5 | 9 | 0 | 11 | 0.359 |
| 676.29 | 57 | 84 | 226 | 41 | 111 | 21 | 247 | 7 | 16 | 26 | 12 | 0.686 |
| 680.99 | 24 | 62 | 129 | 73 | 131 | 40 | 184 | 3 | 12 | 32 | 12 | 0.388 |
| 685.33 | 21 | 46 | 111 | 40 | 90 | 26 | 144 | 7 | 0 | 34 | 11 | 0.447 |
| 686.49 | 16 | 36 | 118 | 37 | 90 | 24 | 144 | 3 | 0 | 42 | 12 | 0.450 |
| 691.11 | 23 | 62 | 190 | 70 | 147 | 41 | 165 | 9 | 11 | 16 | 10 | 0.368 |
| 696.37 | 36 | 89 | 134 | 75 | 181 | 44 | 200 | 7 | 14 | 29 | 11 | 0.403 |
| 696.74 | 22 | 52 | 33 | 52 | 123 | 33 | 231 | 7 | 30 | 16 | 15 | 0.427 |
| 704.84 | 46 | 105 | 187 | 67 | 140 | 34 | 252 | 10 | 17 | 21 | 9 | 0.440 |
| 708.45 | 27 | 73 | 146 | 51 | 126 | 36 | 211 | 6 | 13 | 28 | 13 | 0.363 |
| 710.63 | 43 | 91 | 175 | 53 | 127 | 30 | 228 | 4 | 14 | 23 | 10 | 0.475 |
| 715.50 | 23 | 70 | 185 | 74 | 150 | 41 | 165 | 8 | 8 | 18 | 9 | 0.325 |
| 720.87 | 36 | 104 | 179 | 72 | 172 | 42 | 201 | 10 | 22 | 20 | 10 | 0.341 |
| 724.05 | 30 | 86 | 176 | 69 | 147 | 39 | 181 | 5 | 0 | 16 | 9 | 0.349 |
| 730.84 | 25 | 66 | 150 | 84 | 170 | 40 | 188 | 12 | 16 | 28 | 11 | 0.377 |
| 735.36 | 33 | 92 | 235 | 69 | 156 | 34 | 183 | 12 | 17 | 17 | 9 | 0.362 |
| 737.32 | 22 | 65 | 125 | 86 | 168 | 36 | 185 | 9 | 13 | 0 | 12 | 0.343 |
| 740.86 | 20 | 66 | 217 | 56 | 133 | 31 | 147 | 15 | 10 | 19 | 10 | 0.302 |
| 744.85 | 26 | 71 | 113 | 51 | 123 | 30 | 233 | 11 | 12 | 0 | 14 | 0.362 |
| 750.04 | 40 | 87 | 167 | 46 | 113 | 26 | 254 | 10 | 5 | 34 | 11 | 0.457 |
| 754.84 | 23 | 60 | 86 | 38 | 102 | 25 | 189 | 8 | 1 | 0 | 12 | 0.382 |
| 759.71 | 51 | 107 | 153 | 64 | 136 | 33 | 233 | 6 | 0 | 16 | 10 | 0.479 |
| 765.03 | 34 | 68 | 186 | 85 | 183 | 32 | 211 | 6 | 15 | 0 | 15 | 0.491 |
| 770.23 | 35 | 87 | 134 | 56 | 135 | 29 | 216 | 6 | 14 | 52 | 12 | 0.403 |
| 776.58 | 21 | 49 | 130 | 27 | 85 | 21 | 135 | 8 | 23 | 18 | 11 | 0.424 |
| 777.67 | 27 | 53 | 112 | 47 | 111 | 26 | 162 | 9 | 11 | 5 | 12 | 0.512 |
| 780.51 | 9 | 26 | 73 | 16 | 38 | 11 | 86 | 1 | 0 | 43 | 9 | 0.358 |
| 787.68 | 51 | 81 | 133 | 71 | 131 | 31 | 181 | 5 | 21 | 14 | 10 | 0.624 |

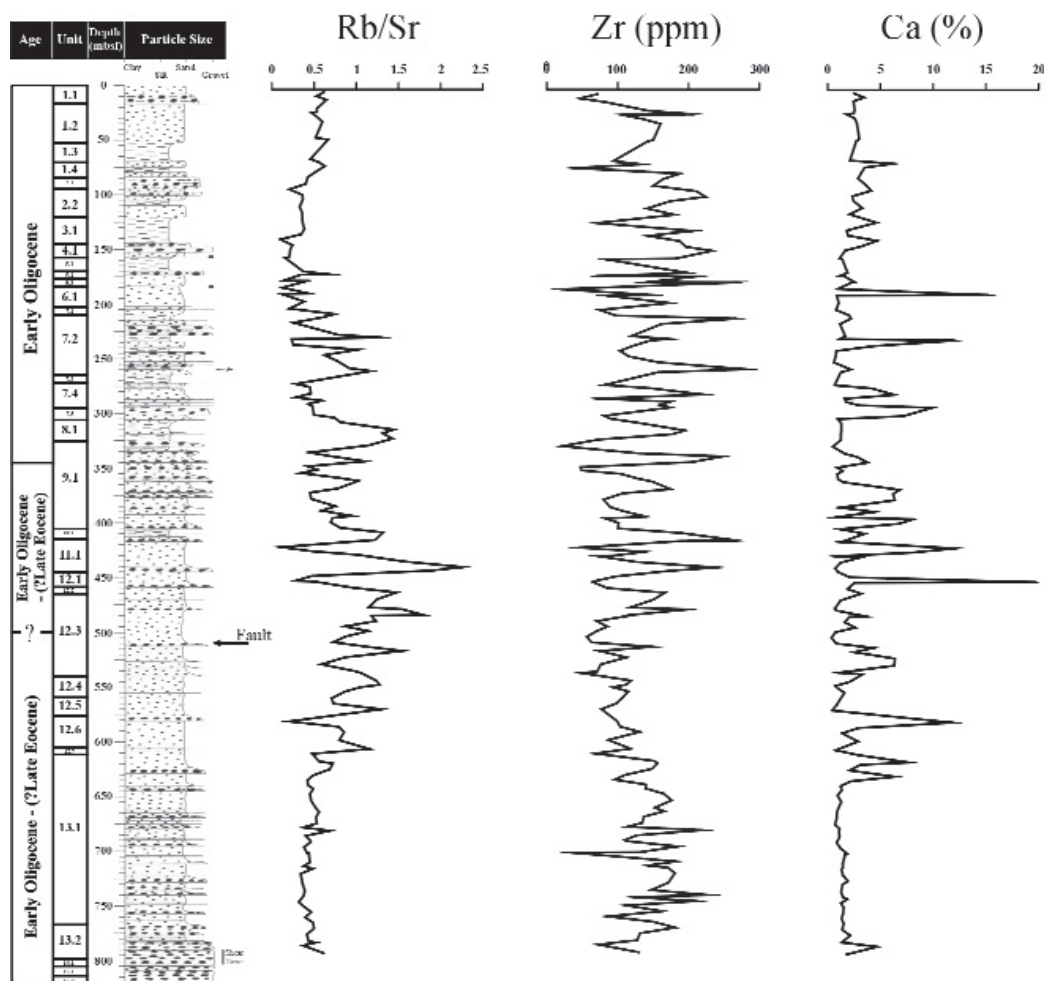


Fig. 2 - CRP-3 lithologic section with depth profiles for Rb/Sr, Zr, and Ca. Symbols as in figure 1.

core (0-340 mbsf) the periodicity previously recognized in different sedimentary physical properties by Cape Roberts Team (2000). These scientists estimated that the short-eccentricity orbital component can be recorded in the magnetic susceptibility and porosity signals of the upper part of CRP-3 and calculated a wavelength of about 5.8-9.7m for this orbital periodicity band. Such a result highlights that the sampling rate adopted for the geochemical analysis of the whole core (average of 1 sample/5 m) is lower than the Nyquist frequency and that all the classic Milankovitch periodicities are not identifiable in the geochemical records.

For the lower part of the CRP-3 core (below 340 mbsf), poorly constrained biostratigraphic and palaeomagnetic data, together with the presence of possible sedimentary hiatuses and abrupt variations of the sedimentation rate, limit the interpretation of the results of the spectral analyses. However, a preliminary study of the dominant periodicities characterizing selected geochemical signals is here proposed taking into account that the obtained results have to be considered only as pilot tools for further researches.

A two steps strategy has been adopted to interpret

the results of spectral analysis.

Power spectra have been estimated in the space domain on selected geochemical signals. Hierarchical patterns among the dominant periodicity bands recorded in the spectra have been compared with the ratios measured among the three Milankovitch frequencies (related to the precession, obliquity and eccentricity cycles) during the Cenozoic in order to preliminarily verify a hypothetical interaction between the studied cyclical sedimentary system and the orbital forcing.

Then, an average sedimentation rate has been estimated for the interval 340.8-627.3 mbsf, characterized by the palaeomagnetic chron C13n (Florindo et al., this volume) which covers the time interval between 33.058 and 33.545 Ma (Cande and Kent, 1995). The estimated average sedimentation rate allowed the transformation of the main frequency peaks present in the spectra (space domain) in time periodicities (time domain).

NUMERICAL METHODOLOGY

Data have been re-sampled with a 5 m constant rate using a cubic spline interpolation method to

avoid high frequency bias on the original data.

Long-term trends have been previously subtracted to the original record by means of a 5 points Gaussian filter.

Welch's averaged periodogram method (Welch, 1967) was used for the estimation of the Fourier Power Spectra.

POWER SPECTRA, NUMERICAL FILTERING AND ORBITALLY-CONTROLLED SEDIMENTARY PROCESSES

Data of SiO₂, Rb/Sr, and Ni for the CRP-3 drillhole have been processed by spectral analyses. These three geochemical signals have been chosen because they appear to be good tracers of sediment provenance for the studied area (see above). In particular, higher SiO₂ values and Rb/Sr ratios are thought to indicate a dominant Beacon Supergroup influence, whereas higher Ni contents should represent a more significant detrital input from the Ferrar Supergroup.

In the power spectra (Fig. 3), the y-axis indicates the variance associated to each harmonic component, while the x-axis refers to frequencies in cycles/meter. Peaks that are statistically significant (passing the 95% confidence level) are labelled with length of periodicity in meters.

The power spectra estimated for the three signals, in the 340-789.77 mbsf interval, show a very similar frequency structure and the presence of three main peaks at about 0.003, 0.029, and 0.052 cycles/meter (Fig. 3). The high variance and quite narrow frequency bands present in the spectra suggest a clear cyclic forcing process, which might have modulated the sedimentary record and the relative geochemical records. Moreover, the spectral results demonstrate the existence of a regular cyclic pattern in the studied

signals and allow us to discard a stochastic mechanism as a controlling factor of their fluctuations.

If we normalize the above-mentioned three frequency bands to the highest one, we obtain a hierarchical pattern (0.058-0.047, 0.36-0.55, 1) similar to that calculated for the classic Milankovitch frequency bands (1/400 cycle/ky for the long-term eccentricity, 1/41-1/54 cycle/ky for the obliquity and 1/19-1/23 cycle/ky for the precession) as indicated by Berger and Loutre (1994) for the Cenozoic.

Such a preliminary result, highlighting a good correspondence of the hierarchical patterns between the two sets of periodicity bands, suggests a possible direct link between astronomical forcing and the sedimentary response in the glaciomarine environment at the margin of the Antarctic Ice Sheet during the early Oligocene.

Considering the average 0.59 m/ky sedimentation rate estimated within the interval characterized by the presence of the chron C13n and assuming it approximately constant along all the lower part of the core (from 340.8 to 789.77 mbsf), we could transform the three frequency peaks (corresponding to the wavelengths of 330, 34, and 19 meters reported in Fig. 3) in periodicities of 560 ky, 57 ky, and 32 ky, respectively. We can hypothesize that the recorded cyclicities are essentially governed by external forcing not strictly related to the Milankovitch astronomical modulation. However, such a hypothesis seems to be discarded considering the good match between the hierarchical patterns calculated among the orbital parameters and the set of periodicities modulating the studied sedimentary record. Alternatively, we could consider the main frequency peaks present in the power spectra as truly corresponding to the orbital periodicities of precession, obliquity and long-eccentricity, respectively. Thus, the observed

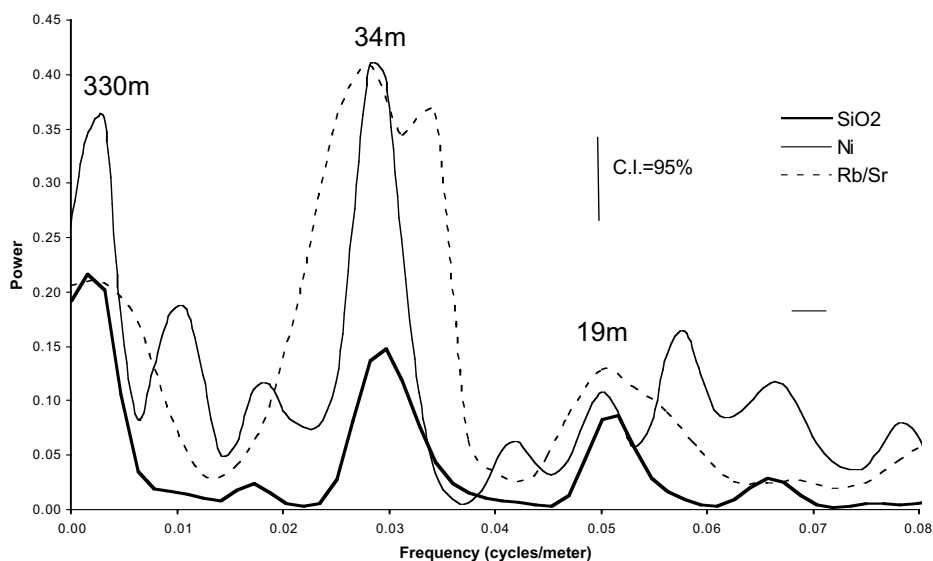


Fig. 3 - Power Spectral Density of three selected geochemical signals (SiO₂, Rb/Sr and Ni) in the 350 to 787 mbsf interval of the CRP-3 core. Main peaks are labelled with the calculated periodicities in metres. B.W. and C.I. represent the Band-Width and the Confidence Interval of the power spectra.

discrepancies between the couples of periodicity bands (in the orbital and sedimentary record) could be explained by hypothesizing that short sedimentary intervals (and, then, time records) are missing. The fault recognized at 539 mbsf (Cape Roberts Science Team, 2000) represents one of the points, along the lower CRP-3 core, where the space/time record could be lost. However, abrupt variations in the sedimentation rate and/or other short intervals of interruption in the sedimentation (not evident by macroscopic analysis of the core) could justify the lack of the records.

In particular, considering the periodicity band of the obliquity and precession cycles and the time span of the palaeomagnetic chron C13n, we can estimate that about 3 obliquity cycles and 8 precession cycles are missing in this segment. The deficiency of other stratigraphic constrains in the lowermost part of the core limits the possibility to evaluate the amount of time missing in this part of the CRP-3 record.

CONCLUSIONS

Distribution of major and trace elements suggests changes in the predominant source of detritus throughout the CRP-3 sequence. The upper 200 mbsf of sediments are characterized by a strong influence of Ferrar Supergroup whereas, between 200 and 600 mbsf, provenance from Devonian Beacon Supergroup detritus becomes dominant. From ~600 down to ~788 mbsf, geochemistry of CRP-3 sediments appears to be again controlled by Ferrar detritus input.

Preliminary results obtained by spectral analyses of three selected geochemical signals (SiO_2 , Rb/Sr and Ni) from the lower 447 mbsf of CRP-3 core suggest that the studied sedimentary system has been mainly forced by the well-known Milankovitch astronomical components of long-term eccentricity, obliquity, and precession. Sediments appear to be influenced by cyclic alternation of Devonian Beacon Supergroup detritus and Ferrar Supergroup materials with consequent modulation of the three long intervals characterized by dominant inputs of the different source rocks. Further detailed researches, supported by a multidisciplinary approach, will enable the identification of the sedimentary mechanisms, which drove the deposition of sediments with periodic alternations of geochemical tracers.

ACKNOWLEDGEMENTS - We are grateful to Massimo Pompilio for his help for obtaining CRP-3 samples. We would like to thank L. Krissek and M. Claps for their reviews of an earlier version of the paper. This research was supported by the Italian *Programma Nazionale di Ricerche in Antartide* (PNRA).

REFERENCES

- Berger A., 1984. Accuracy and frequency stability of the Earth's orbital elements during the Quaternary. In: Berger A.L., Imbrie J., Hays J., Kukla G. & Saltzman B. (eds.), *Milankovitch and Climate, Part 1*, Reidel Publ. Co., Dordrecht, 3-39.
- Berger A. & Loutre M.F., 1994. Astronomical forcing through geological time. In: de Boer P.L. & Smith D.G. (eds.), *Orbital forcing and cyclic sequences*, IAS Special Publication, **19**, 15-24.
- Cande S. & Kent D., 1995. Revised calibration of the geomagnetic polarity time scale for the late Cretaceous and Cenozoic. *J. Geophys. Res.*, **97**, 13917-13951.
- Cape Roberts Science Team, 1999. Studies from the Cape Roberts Project, Ross Sea, Antarctica. Initial Report on CRP-2/2A. *Terra Antartica*, **6**, 1-173.
- Cape Roberts Science Team, 2000. Studies from the Cape Roberts Project, Ross Sea, Antarctica. Initial Report on CRP-3. *Terra Antartica*, **7**, 1-209.
- Claps M., Niessen F. & Florindo F., 2000. High-frequency analysis of physical properties from CRP-2/2a and implication for sedimentation rate. *Terra Antartica*, **7**, 379-388.
- Ehrmann W., 2001. Variations in smectite content and crystallinity in sediments from CRP-3, Victoria Land Basin, Antarctica. This volume.
- Florindo F., Wilson G.S., Roberts A.P., Sagnotti L. & Verosub K.L., 2001. Magnetostratigraphy of late Eocene - early Oligocene strata from the CRP-3 core, Victoria Land Basin, Antarctica. This volume.
- Franzini M., Leoni L. & Saitta M., 1975. Revisione di una metodologia analitica per fluorescenza X basata sulla correzione completa degli effetti di matrice. *Rend. Soc. Ital. Miner. Petrol.*, **21**, 99-108.
- House M.R., 1995. Orbital forcing timescales. In: House M.R. & Gale A.S. (eds.), *Orbital Forcing Timescales and Cyclostratigraphy*, The Geological Society of London, London, 1-18.
- Niessen F., Kopsch K. & Polozek K., 2000. Velocity and porosity from CRP-2/2A Core Logs, Victoria Land Basin, Antarctica. *Terra Antartica*, **7**, 241-253.
- Roser B.P. & Pyne A.R., 1989. Wholerock geochemistry. In: P.J. Barrett (ed.), *Antarctic Cenozoic History from the CIROS-1 Drillhole, McMurdo Sound*, *DSIR Bull.*, **245**, 175-184.
- Smellie J.L., 2001. History of Oligocene erosion, uplift and unroofing of the Transantarctic Mountains deduced from sandstone detrital modes in CRP-3 drillcore, Victoria Land Basin, Antarctica. This volume.
- Welch P.D., 1967, The use of Fast Fourier Transform for the Estimation of Power Spectra: A method based on time averaging over short, modified periodograms. *IEEE trans. Audio and Electroacoustics*, vol. AU-15, no. 2.